The Mechanics of Vacillation

EDWARD N. LORENZ

Massachusetts Institute of Technology[1,2]

(Manuscript received 3 June 1963)

ABSTRACT

The equations governing a symmetrically heated rotating viscous fluid are reduced to a system of fourteen ordinary differential equations, by a succession of approximations. The equations contain two external parameters—an imposed thermal Rossby number and a Taylor number.

Solutions where the flow is purely zonal, and solutions with superposed "steady" waves which progress without changing their shape, are obtained analytically. Additional solutions exhibiting vacillation, where the waves change shape in a regular periodic manner in addition to their progression, and solutions exhibiting irregular nonperiodic flow, are obtained by numerical integration.

For a given imposed thermal Rossby number, the flow becomes more complicated as the Taylor number increases. Exceptions occur at very high Taylor numbers, where the equations become unrealistic because of truncation.

For values of the external parameters where steady-wave solutions are found, solutions with purely zonal flow also exist, but are unstable, Where vacillating solutions are found, steady-wave solutions also exist, but are unstable. A transition between unsymmetric and symmetric vacillation is not associated with the instability of either form of vacillation. It is hypothesized that where irregular nonperiodic solutions are found, vacillating solutions also exist but are unstable.

1. Regimes of flow

The incessant fluctuations of the state of the atmosphere are noted for their irregularity. Exact repetitions, which would make perfect weather forecasting possible by means of analogues, are conspicuously absent. There is considerable doubt as to whether any exact or nearly exact periodic components, other than the annual and diurnal periods and their overtones, occur with detectable amplitude in tropospheric weather data (cf. Shapiro and Ward, 1960). If hidden periodicities really do exist, they are very well hidden.

In this respect atmospheric flow may be contrasted with the thermally forced flow observed in certain laboratory experiments (cf. Fultz *et al.*, 1959). These experiments have frequently been looked upon as models of the atmosphere, but they often fail to show the irregularity found in the atmosphere. In some of Fultz's earlier experiments, a dishpan containing water was rotated about its axis, and heated near its rim and cooled near its center. Rapid rotation with heating of moderate intensity led to a flow with irregular traveling waves somewhat like those in the atmosphere, but slower rotation or stronger heating led to a steady-state symmetrical flow. In later experiments where the flow was restricted to an annular region, Fultz obtained waves which progressed at a uniform rate without changing their shape. Meanwhile Hide (1953), studying the flow in a deep annular region, obtained waves which underwent regular periodic changes in their shape, in addition to their progression. He called this phenomenon *vacillation.*

The flow occurring during the course of any single experiment, after initial transitory effects have had time to disappear, is characterized by a certain number of degrees of freedom—the number of parameters required to specify a single instantaneous flow pattern from among all the patterns occurring during the experiment. Thus a steady symmetric flow has zero degrees of freedom, since it does not vary with time. A flow with uniformly moving waves has one degree of freedom, which may be taken as the absolute longitude of a chosen feature of a wave. A vacillating flow has two degrees of freedom—the longitude of the wave and the phase of the vacillation cycle. The irregular flows appear to have at least three degrees of freedom; in the case of the atmosphere there are presumably many more.

Together, then, the experiments and the atmosphere exhibit at least four distinct regimes of flow; a steady symmetric regime, a steady-wave regime, a vacillating-wave regime, and an irregular-wave regime. We shall refer to these regimes respectively as $\mathcal{R}_0$,$\mathcal{R}_1$, $\mathcal{R}_2$ and $\mathcal{R}_{3+}$, the subscript indicating the number of degrees of freedom. Presumably $\mathcal{R}_{3+}$ may be further subdivided. Regime $\mathcal{R}_0$ is called the *Hadley regime*, while $\mathcal{R}_1$, $\mathcal{R}_2$ and

[1] The research reported in this work has been sponsored in part by the Air Force Cambridge Research Laboratories, under contract AF 19(604)-4969.

[2] A portion of this work was performed while the writer was at the National Center for Atmospheric Research, Boulder, Colo.

$\mathcal{R}_{3+}$ together form the *Rossby regime*, which might, in our notation, be denoted by $\mathcal{R}_{1+}$. Regime $\mathcal{R}_1$ will be called the *steady Rossby regime*, and the waves occurring in it, which appear steady in a suitably moving coordinate system, will be called *steady waves*.

In attempting to account for the occurrence of both the Hadley and the Rossby regimes in a single experimental apparatus, the writer (1953) advanced the hypothesis that steady symmetric flow is mathematically possible under all combinations of rotation and symmetric heating, but that under certain combinations this symmetric flow is unstable with respect to wave disturbances of small amplitude. Waves generated by the inevitable small-amplitude irregularities will therefore attain appreciable size, and symmetric flow will not be observed experimentally in these instances.

In a more recent study, hereafter referred to as S, the writer (1962) attempted to substantiate this hypothesis with a simple dynamic model. In this model, steady Hadley flow proved to be always possible. The instability of this flow proved to be a sufficient, but not a necessary, condition for the occurrence of a Rossby flow. For a given low value of the heating, the corresponding critical rate of rotation for the development of small-amplitude waves proved to be the same as the critical rate for the disappearance of already-established waves, but for high values of the heating, the two criteria were not the same. Thus there were combinations of heating and rotation for which a Hadley flow and a well developed Rossby flow represented alternative stable states.

Guided by these considerations, we may attempt to account for the occurrence of vacillation, and of regimes with three or more degrees of freedom. We hypothesize that when the Hadley circulation is unstable, at least one steady Rossby circulation is mathematically possible. Under certain conditions one or more of these Rossby circulations may be unstable with respect to still further disturbances. If all the steady Rossby circulations are unstable, none will be observed experimentally, and the system will oscillate with at least two degrees of freedom. It should be emphasized that the instability of a Rossby circulation means the instability of the entire flow configuration, and not just the instability of the zonal part alone.

We further hypothesize that when the Hadley circulation and all the steady Rossby circulations are unstable, at least one Rossby circulation with just two degrees of freedom, i.e., a vacillating circulation, is mathematically possible. If at least one vacillating circulation is stable, vacillation may be observed experimentally. If all the vacillating circulations are unstable, the system will oscillate with at least three degrees of freedom.

Finally, vacillation may be possible even when a steady Rossby circulation is stable, provided that the criterion for the development of a second degree of freedom differs from the criterion for the disappearance of an already established second degree of freedom.

As in S, we shall attempt to substantiate our hypotheses with a simple dynamic model. In S, a system of eight ordinary differential equations proved sufficient to describe the essential features of the transition between the Hadley and Rossby regimes, and between distinct Rossby regimes characterized by distinct wave numbers. These equations did not appear capable, however, of describing the phenomenon of vacillation. In this study, we shall use a slightly less drastic simplification, which will yield a system of fourteen ordinary differential equations. The phenomenon of vacillation will then be exhibited through the use of numerical integration.

Throughout the study, we shall be primarily concerned with the mechanism via which vacillation arises, rather than the specific values of rotation and heating which can lead to vacillation. If we were interested in duplicating the results of the laboratory experiments as closely as we were able to duplicate them in S, we should probably have to work with still less drastically simplified equations.

2. The spectral form of the two-layer model

Among the simplest systems of equations capable of depicting the prominent features of baroclinic flow are the geostrophic and quasigeostrophic "numerical weather prediction" models. One of the most feasible means of further simplifying these models consists of expanding each variable in an appropriate series of orthogonal functions, and then truncating each series to include only a specified set of orthogonal functions. The coefficients of these functions, which become the dependent variables in the new system of equations, may be regarded as forming generalized spectral analyses of the original variables. In this section we shall derive a general spectral form for one of the numerical-prediction models. In the following section the equations will be specialized for the vacillation problem. Meanwhile, the general form will remain available for other studies of this sort.

In the geostrophic form of the two-layer model described by the writer (1960), we denote the stream functions for the nondivergent part of the horizontal flow in the upper and lower layers by $\psi+\tau$ and $\psi-\tau$, the temperatures (in the case of a liquid) or potential temperatures (in the case of a gas) in these layers by $\theta+\sigma$ and $\theta-\sigma$, and the velocity potentials for the irrotational part of the horizontal flow in these layers by $-\chi$ and χ. The domain of these functions may be unbounded, like the surface of a sphere, or there may be boundaries across which no mass flows, in which case the tangential derivatives of ψ and τ, and the normal derivative of χ, vanish at the boundaries. If we take the Coriolis parameter f to be constant, and further simplify the system

by letting the static stability σ vary only with time, and not in the horizontal directions, the equations of the model simplify to

$$\partial\nabla^2\psi/\partial t=-J(\psi,\nabla^2\psi)-J(\tau,\nabla^2\tau), \tag{1}$$

$$\partial\nabla^2\tau/\partial t=-J(\psi,\nabla^2\tau)-J(\tau,\nabla^2\psi)+f\nabla^2\chi, \tag{2}$$

$$\partial\theta/\partial t=-J(\psi,\theta)+\bar{\sigma}\nabla^2\chi, \tag{3}$$

$$\partial\bar{\sigma}/\partial t=-\overline{\theta\nabla^2\chi}. \tag{4}$$

Here t is time, J denotes a Jacobian with respect to horizontal coordinates, and a bar denotes a horizontal average. The system is rendered closed by the thermal wind equation

$$\nabla^2\theta=A\nabla^2\tau, \tag{5}$$

where A is a constant whose value depends upon the properties of the fluid, and, in particular, upon whether the fluid is a liquid or a gas.

Still further simplifications would result from neglecting the time variations of $\bar{\sigma}$. The system would then reduce to one of the conventional two-layer models, the original example of which was given by Phillips (1951).

To transform these equations into spectral form, we determine a denumerable set of *orthogonal functions* $F_0, F_1, F_2, \cdots$ which satisfy the following conditions:

$$L^2\nabla^2F_i=-a_i^2F_i, \quad i=0, 1, \cdots, \tag{6}$$

where L is a constant with the dimensions of distance,

$$\partial F_i/\partial s=0, \quad i=0, 1, \cdots \tag{7}$$

everywhere on the boundary, if a boundary exists, $\partial/\partial s$ denoting a tangential derivative, and

$$\overline{F_iF_j}=\delta_{ij}\equiv\begin{cases}1 & \text{if} \quad i=j,\\ 0 & \text{if} \quad i\neq j.\end{cases} \tag{8}$$

We shall furthermore require that $F_0\equiv 1$, whence $a_0=0$.

The Jacobian of two orthogonal functions will satisfy the relation

$$L^2J(F_j,F_k)=\sum_{i=0}^{\infty}c_{ijk}F_i, \tag{9}$$

where

$$c_{ijk}=L^2\overline{F_iJ(F_j,F_k)}. \tag{10}$$

It is evident that $c_{ijk}=-c_{ikj}$. From the boundary condition (7) it follows that $c_{ijk}=c_{jki}=c_{kij}$.

We now introduce the expansions

$$\psi=L^2f\sum_{i=1}^{\infty}\psi_iF_i, \tag{11}$$

$$\tau=L^2f\sum_{i=1}^{\infty}\tau_iF_i, \tag{12}$$

$$\theta=AL^2f\sum_{i=0}^{\infty}\theta_iF_i, \tag{13}$$

$$\bar{\sigma}=AL^2f\sigma_0. \tag{14}$$

A similar expansion for χ is not permissible since χ satisfies different boundary conditions. However, since only $\nabla^2\chi$ appears in (1)–(4), we may let

$$\nabla^2\chi=f\sum_{i=1}^{\infty}\omega_iF_i. \tag{15}$$

The coefficients ψ_i, τ_i, θ_i, σ_0, and ω_i are dimensionless. In essence, we have used L as the unit of distance and f^{-1} as the unit of time.

When relations (11)–(15) are substituted into (1)–(4), and the coefficients of like orthogonal functions are equated, we find that

$$\dot{\psi}_i=\tfrac{1}{2}\sum_{j,k=1}^{\infty}a_i^{-2}(a_j^2-a_k^2)c_{ijk}(\psi_j\psi_k+\tau_j\tau_k), \tag{16}$$

$$\dot{\tau}_i=\tfrac{1}{2}\sum_{j,k=1}^{\infty}a_i^{-2}(a_j^2-a_k^2)c_{ijk}(\tau_j\psi_k+\psi_j\tau_k)-a_i^{-2}\omega_i, \tag{17}$$

$$\dot{\theta}_i=\tfrac{1}{2}\sum_{j,k=1}^{\infty}c_{ijk}(\theta_j\psi_k-\psi_j\theta_k)+\sigma_0\omega_i, \tag{18}$$

$$\dot{\sigma}_0=-\sum_{i=1}^{\infty}\theta_i\omega_i, \tag{19}$$

while, in view of (5),

$$\theta_i=\tau_i \quad \text{if} \quad a_i\neq 0. \tag{20}$$

Here a dot denotes a derivative with respect to a dimensionless time $t_0=ft$. The coefficients $\frac{1}{2}$ before the double summations can be omitted if the summations are taken over only those pairs (j,k) for which $k>j$, thus eliminating repetitions. Equations (16)–(20) are the general spectral form of equations (1)–(5).

The particular set of functions F_i to be used in any given problem depends upon the domain of the variables ψ, τ, θ, σ, and χ. However, the functions F_i enter equations (16)–(20) only through the coefficients a_i and c_{ijk}. All that need be stated concerning the domain are therefore the values of a_i, and of c_{ijk} for those triples (i,j,k) for which $c_{ijk}\neq 0$. If two geometrically different domains happen to lead to the same coefficients a_i and c_{ijk}, they will lead to identical spectral forms of the two-layer model.

The equations so far presented apply to the "adiabatic" form of the two-layer model, in which forcing and dissipation of a mechanical or thermal nature are omitted. In many studies, including the present one, it is essential to include these processes. A number of schemes for this purpose are possible; a simple one is given in S. Here there is assumed a frictional drag at

the lower surface, proportional to the velocity in the lower layer, and a frictional drag at the surface separating the two layers, proportional to the shear at this surface. Likewise there is assumed a heating of the lower layer, proportional to the difference between the temperature (or potential temperature) of the lower layer and a preassigned temperature field θ^*, and a heat exchange between the layers, proportional to the difference between the temperatures of the layers. The expansion for θ^* is obtained by adding stars to equation (13). If the coefficients of friction at the lower surface and the surface separating the layers, after being made dimensionless by dividing by f, are denoted by $2k$ and k', and if the dimensionless coefficients of heating at these surfaces are denoted by $2h$ and h', the *additional* terms in the spectral form of the model become

$$\dot{\psi}_i = -k(\psi_i - \tau_i), \tag{21}$$

$$\dot{\tau}_i = k\psi_i - (k+2k')\tau_i, \tag{22}$$

$$\dot{\theta}_i = -h(\theta_i - \sigma_i) + h\theta_i^*, \tag{23}$$

$$\dot{\sigma}_0 = h\theta_0 - (h+2h')\sigma_0 - h\theta_0^*. \tag{24}$$

Other assumptions concerning the nonadiabatic effects are possible. For example, a heat exchange between the upper layer and the environment might be added.

3. The equations of the specific model

In order to apply the general spectral equations to a specific problem, we need to specify the values of the constants a_i and c_{ijk}. These values are determined by the orthogonal functions F_i. The appropriate choice for the functions F_i depends upon the geometry of the domain of the flow.

In S this domain was taken to be a circular cylindrical region, and the variables were expanded in Fourier-Bessel series. In the present study it might be more logical to use an annular region, since it is in such a region that vacillation is most readily observed experimentally.

Still another region, which is difficult to set up experimentally, but is much simpler mathematically, and has often been used to approximate the annulus, is the infinite channel, in which the flow is required to vary periodically along the length, with a specified fundamental wavelength. In this study we shall choose the infinite channel as the domain of the flow.

If our hypothesis concerning vacillation is correct, vacillation should be mathematically possible in a cylindrical as well as an annular domain. It may, however, be unstable with respect to further modes of oscillation, in the cylinder. Possibly these modes are not admitted by the geometry of the annulus. In a study using truncated series of orthogonal functions, whether the domain be a cylinder, an annulus, or an infinite channel, we can suppress various troublesome modes simply by not including the orthogonal functions necessary to describe them. Hence the vacillation which we shall demonstrate numerically in the infinite channel could perhaps just as readily be demonstrated in an annulus or a cylinder.

Introducing rectangular coordinates x and y, we shall let the walls of the channel be the surfaces $y=0$ and $y=\pi L$. A suitable set of orthogonal functions is then the set

$$\phi_{00} = 1, \tag{25}$$

$$\phi_{0m} = \sqrt{2}\cos my_0, \tag{26}$$

$$\phi_{nm} = 2\sin my_0 \cos nx_0, \tag{27}$$

$$\phi_{nm}' = 2\sin my_0 \sin nx_0, \tag{28}$$

where $x_0 = x/L$ and $y_0 = y/L$. These functions form a denumerable set, and so may be identified with the functions F_i in the general spectral form of the equations.

We next truncate the series expansions (11)–(15) for ψ, τ, θ, σ, and $\nabla^2\chi$ by retaining only those orthogonal functions (26)–(28) with $m=1$ or 2, and with a single value of n. We shall find it convenient to use capital letters instead of numbers for the subscripts of specific orthogonal functions F_i, and the associated constants and variables a_i, c_{ijk}, ψ_i, τ_i, θ_i, ω_i and θ_i^*. Thus we shall let $\phi_{00}=F_0$, $\phi_{01}=F_A$, $\phi_{n1}=F_K$, $\phi_{n1}'=F_L$, $\phi_{02}=F_C$, $\phi_{n2}=F_M$, and $\phi_{n2}'=F_N$. The functions F_A and F_C represent the zonal portion of the flow, while F_K, F_L F_M, and F_N represent superposed waves. We shall call a wave represented by F_K and F_L a wave of the *first mode*, and one represented by F_M and F_N a wave of the *second mode*. ("Mode" thus refers to the form of the y-variation.)

For the preassigned temperature field θ^*, we use the simpler expansion

$$\theta^* = AL^2 f(\theta_0^* + \theta_A^* F_A). \tag{29}$$

We observe that $a_A{}^2=1$, $a_K{}^2=a_L{}^2=n^2+1$, $a_C{}^2=4$, and $a_M{}^2=a_N{}^2=n^2+4$. The only triples (i,j,k) for which c_{ijk} does not vanish are (A,K,L), (A,M,N), (C,K,N), *and* (C,M,L). We find from (10) that

$$\frac{c_{AKL}}{5} = \frac{c_{AMN}}{4} = \frac{c_{CKN}}{8} = \frac{c_{CML}}{8} = -\frac{8\sqrt{2}}{15\pi}n. \tag{30}$$

We introduce the further symbols

$$\beta = a_K{}^{-2}(a_L{}^2 - a_A{}^2) = n^2/(n^2+1),$$

$$\beta' = a_M{}^{-2}(a_N{}^2 - a_A{}^2) = (n^2+3)/(n^2+4),$$

$$\delta = a_K{}^{-2}(a_N{}^2 - a_C{}^2) = n^2/(n^2+1),$$

$$\delta' = a_N{}^{-2}(a_L{}^2 - a_C{}^2) = (n^2-3)/(n^2+4),$$

and

$$\epsilon = a_C{}^{-2}(a_M{}^2 - a_L{}^2) = \tfrac{3}{4}.$$

Letting $\alpha = -c_{AKL}$, $\alpha' = -c_{AMN}$, and $\alpha'' = -c_{CKN} = -c_{CML}$, we obtain the equations

$$\dot{\psi}_A = -k(\psi_A-\theta_A) \tag{31}$$

$$\dot{\psi}_K = -\beta\alpha(\psi_L\psi_A+\theta_L\theta_A) - \delta\alpha''(\psi_N\psi_C+\theta_N\theta_C) - k(\psi_K-\theta_K) \tag{32}$$

$$\dot{\psi}_L = \beta\alpha(\psi_A\psi_K+\theta_A\theta_K) + \delta\alpha''(\psi_C\psi_M+\theta_C\theta_M) - k(\psi_L-\theta_L) \tag{33}$$

$$\dot{\psi}_C = \epsilon\alpha''(\psi_K\psi_N+\theta_K\theta_N) - \epsilon\alpha''(\psi_M\psi_L+\theta_M\theta_L) - k(\psi_C-\theta_C) \tag{34}$$

$$\dot{\psi}_M = -\beta'\alpha'(\psi_N\psi_A+\theta_N\theta_A) - \delta'\alpha''(\psi_L\psi_C+\theta_L\theta_C) - k(\psi_M-\theta_M) \tag{35}$$

$$\dot{\psi}_N = \beta'\alpha'(\psi_A\psi_M+\theta_A\theta_M) + \delta'\alpha''(\psi_C\psi_K+\theta_C\psi_K) - k(\psi_N-\theta_N) \tag{36}$$

$$\dot{\theta}_A = -\omega_A+k\psi_A-(k+2k')\theta_A \tag{37}$$

$$\dot{\theta}_K = -\beta\alpha(\theta_L\psi_A+\psi_L\theta_A) - \delta\alpha''(\theta_N\psi_C+\psi_N\theta_C) - (1-\beta)\omega_K + k\psi_K - (k+2k')\theta_K \tag{38}$$

$$\dot{\theta}_L = \beta\alpha(\theta_A\psi_K+\psi_A\theta_K) + \delta\alpha''(\theta_C\psi_M+\psi_C\theta_M) - (1-\beta)\omega_L + k\psi_L - (k+2k')\theta_L \tag{39}$$

$$\dot{\theta}_C = \epsilon\alpha''(\theta_K\psi_N+\psi_K\theta_N) - \epsilon\alpha''(\theta_M\psi_L+\psi_M\theta_L) - (1-\epsilon)\omega_C + k\psi_C - (k+2k')\theta_C \tag{40}$$

$$\dot{\theta}_M = -\beta'\alpha'(\theta_N\psi_A+\psi_N\theta_A) - \delta'\alpha''(\theta_L\psi_C+\psi_L\theta_C) - (1-\beta')\omega_M + k\psi_M - (k+2k')\theta_M \tag{41}$$

$$\dot{\theta}_N = \beta'\alpha'(\theta_A\psi_M+\psi_A\theta_M) + \delta'\alpha''(\theta_C\psi_K+\psi_C\theta_K) - (1-\beta')\omega_N + k\psi_N - (k+2k')\theta_N \tag{42}$$

$$\dot{\theta}_0 = -h\theta_0 + h\sigma_0 + h\theta_0^* \tag{43}$$

$$\dot{\theta}_A = -\alpha(\theta_K\psi_L-\psi_K\theta_L) - \alpha'(\theta_M\psi_N-\psi_M\theta_N) + \sigma_0\omega_A - h\theta_A + h\theta_A^* \tag{44}$$

$$\dot{\theta}_K = -\alpha(\theta_L\psi_A-\psi_L\theta_A) - \alpha''(\theta_N\psi_C-\psi_N\theta_C) + \sigma_0\omega_K - h\theta_K \tag{45}$$

$$\dot{\theta}_L = -\alpha(\theta_A\psi_K-\psi_A\theta_K) - \alpha''(\theta_C\psi_M-\psi_C\theta_M) + \sigma_0\omega_L - h\theta_L \tag{46}$$

$$\dot{\theta}_C = -\alpha''(\theta_K\psi_N-\psi_K\theta_N) - \alpha''(\theta_M\psi_L-\psi_M\theta_L) + \sigma_0\omega_C - h\theta_C \tag{47}$$

$$\dot{\theta}_M = -\alpha'(\theta_N\psi_A-\psi_N\theta_A) - \alpha''(\theta_L\psi_C-\psi_L\theta_C) + \sigma_0\omega_M - h\theta_M \tag{48}$$

$$\dot{\theta}_N = -\alpha'(\theta_A\psi_M-\psi_A\theta_M) - \alpha''(\theta_C\psi_K-\psi_C\theta_K) + \sigma_0\omega_N - h\theta_N \tag{49}$$

$$\dot{\sigma}_0 = -(\theta_A\omega_A+\theta_K\omega_K+\theta_L\omega_L+\theta_C\omega_C+\theta_M\omega_M+\theta_N\omega_N) + h\theta_0 - (h+2h')\sigma_0 - h\theta_0^* \tag{50}$$

Altogether there are 20 equations. However the six variables ω_A, ω_K, $\cdots$ are easily eliminated. There then remains a set of 14 ordinary differential equations in 14 variables. In the remainder of this paper we shall be concerned with solutions of this set of equations.

4. Analytic solutions

Equations (31)–(50), although presented as a simplified system, are still so complicated that a general solution, or even the most general statistically stationary solution, cannot readily be found analytically. Nevertheless, certain analytic solutions are easily obtained. In this section we shall present analytic solutions for the Hadley circulations, and for some of the steady Rossby circulations. We shall then examine these solutions for stability with respect to further modifications of small amplitude.

The coefficients k, k', h, and h' were made dimensionless through division by f. As in S, we shall arbitrarily fix the ratios of these coefficients, and let $h'=k'=h/2=k/2$. The controllable external parameters may then be taken as θ_A^* and k.

Seeking first the steady Hadley circulation, we observe that if all the variables with subscripts K, L, M, or N vanish identically, the equations governing these variables are automatically satisfied. The equations governing ψ_C and θ_C then show that ψ_C and θ_C also vanish in a steady-state solution. The equations governing ψ_A, θ_0, θ_A, and σ_0 may then be readily solved for their steady-state values. The steady Hadley circulation is identical with the one determined in S; specifically

$$\psi_A = \theta_A, \tag{51}$$

$$\theta_0 = \theta_0^* + \theta_A^2, \tag{52}$$

$$\sigma_0 = \theta_A^2, \tag{53}$$

while θ_A is the single real root of the cubic equation

$$\theta_A + \theta_A^3 = \theta_A^*. \tag{54}$$

As indicated in S, ψ_A and θ_A are proportional, respectively, to the *Rossby number* and the *thermal Rossby number*. The ratio

$$R = \sigma_0/\theta_A^2 \tag{55}$$

is proportional to the *Richardson number*, so that the entire steady Hadley regime is characterized by a single Richardson number. The external parameter θ_A^* is proportional to the *imposed thermal Rossby number*,

while k^{-2} is proportional to the *Taylor number*. Under the physical assumption that the coefficient of friction does not vary greatly from one experiment to another, k^{-1} becomes a measure of the rate of rotation.

We next observe that if all the quantities with subscripts C, M, or N vanish identically, the equations governing these same quantities are automatically satisfied. The remaining equations are then formally identical with the entire set considered in S. The steady Rossby circulations determined in S are therefore to be found among the steady Rossby circulations satisfying equations (31)–(50). These circulations contain waves of the first mode only, and we shall call them *Rossby circulations of the first mode.* Incidentally, this result would not hold if θ_C^* had not been taken equal to zero in (29).

The following equations describing these circulations are taken directly from S. For a Rossby circulation of the first mode,

$$\theta_A=\alpha^{-1}kG(\sigma_0), \tag{56}$$

where

$$G^2(\sigma_0)=(2+3s)^3[(6\beta-\beta^2)+(11\beta-6\beta^2)s+(3\beta-6\beta^2)s^2-5\beta^2s^3]^{-1} \tag{57}$$

and

$$s=(1-\beta)^{-1}\sigma_0. \tag{58}$$

Equations (53) and (54), which hold for Hadley circulations, and (56), which holds for Rossby circulations, together form the critical conditions for the stability of a steady Hadley flow with respect to waves of the first mode.

For an established Rossby circulation of the first mode,

$$\psi_K=B\cos\omega(t-t_{00}), \tag{59}$$

$$\psi_L=B\sin\omega(t-t_{00}), \tag{60}$$

$$\theta_K=p\psi_K+q\psi_L, \tag{61}$$

$$\theta_L=-q\psi_K+p\psi_L, \tag{62}$$

where t_{00} is arbitrary,

$$\omega=k(1+5s)(2+3s)^{-1}\beta G, \tag{63}$$

$$p=(1+\beta^2G^2)^{-1}[1-(1-2s)(2+3s)^{-1}\beta^2G^2], \tag{64}$$

and

$$q=(1+\beta^2G^2)^{-1}(3+s)(2+3s)^{-1}\beta G \tag{65}$$

are functions of σ_0 alone, and

$$B^2=(qG-p^2-q^2)^{-1}\sigma_0(\sigma_0-\theta_A^2). \tag{66}$$

Equations (57)–(66) relate the Rossby circulation to θ_A and σ_0; it is related to θ_A^* and k through (56) and the further relation

$$\theta_A^*=\theta_A[1+\sigma_0(qG-p^2-q^2)^{-1}(RqG-p^2-q^2)]. \tag{67}$$

We now observe that if all the quantities with subscripts C, K or L vanish identically, the equations governing these quantities are automatically satisfied, and the remaining equations are again formally identical with the set solved in S, with α and β replaced by α' and β'. There is therefore a second set of steady Rossby circulations satisfying equations (31)–(50). These circulations contain waves of the second mode only, and will be called *Rossby circulations of the second mode.* The equations describing them are obtained by replacing the subscripts K and L by M and N, and by adding primes to α, β, G, s, ω, p, q, and B, in equations (56)–(67).

In Fig. 1, the two heavy solid curves labeled "1" and "2" represent critical conditions for the stability of the steady Hadley flow with respect to wave disturbances of the first and second modes, respectively, for the case $n=2$. For this case, $\alpha=2.40$, $\alpha'=1.92$, $\beta=\frac{4}{5}$, and $\beta'=\frac{7}{8}$. The coordinates are k^{-2} and θ_A^*, on logarithmic scales. The area to the right of each curve indicates the region of instability.

We observe that curve "2" lies completely on the concave side of the curve "1." Hence there are no Hadley circulations unstable with respect to waves of the second mode which are not also unstable with respect to waves of the first mode. Thus, if a stable Hadley circulation is established, and then k^{-2} and θ_A^* are altered in the direction of instability, waves of the first mode will appear first. This situation is not the result of choosing $n=2$, but must occur whenever $\alpha>\alpha'$ and $\beta<\beta'$. These inequalities hold for every value of n. This result, incidentally, is unlike the result obtained when two different values of n are permitted together, as in the latter portion of S, where the critical curves are found to intersect.

The value $n=2$ indicates a wave length πL. If, in an analogy between the channel and the cylinder, the

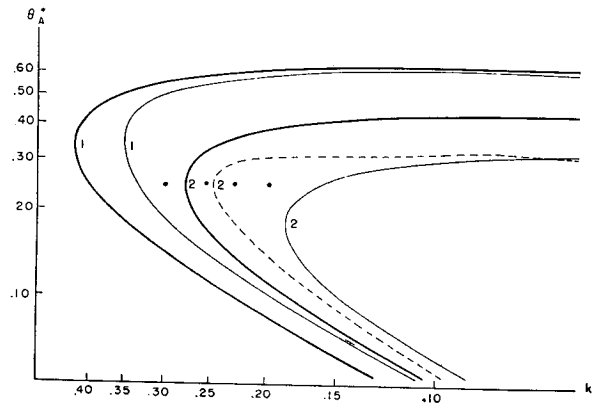

FIG. 1. Critical curves for the instability of established regimes of flow. Heavy curves 1 and 2: Instability of Hadley flow with respect to waves of first and second modes. Thin solid curves 1 and 2: Instability of Rossby flow of first and second modes with respect to waves of second and first modes. Dashed curve 2: Overstability of Rossby flow of second mode with respect to waves of first mode. Dots locate the numerical solutions of Tables 1–5.

width πL of the channel is identified with the radius of the cylinder, wave-length πL in the channel corresponds to some wave number smaller than 2π, whose exact value depends upon how far from the center of the cylinder one chooses to measure the length of a wave. Actually the values $\alpha=2.4$ and $\beta=0.8$ correspond most closely to the value of α for wave number 8 and the value of β for wave number 5, as tabulated in S. In an analogy between the channel and the annulus, πL may be identified with the width of the annulus, and wave-length πL may correspond to a much higher wave number, if the annulus is narrow.

We note, in passing, that the results presented in S would not have been altered, except for changes in the numerical values of α and β, if the cylindrical region used in S had been replaced by the infinite channel. It does not follow, however, that the results of the present study would be unaltered by replacing the infinite channel by a cylinder, or an annulus. The choice of the channel has made the coefficients c_{AKN}, c_{AML}, c_{CKL}, and c_{CMN} all equal to zero; the corresponding coefficients in the case of the cylinder or the annulus do not vanish. Thus the two distinct Rossby circulations which we have found in the channel would assume more complicated expressions in the annulus or the cylinder (if they exist there at all as distinct circulations), since each circulation would involve waves of both modes. A similar situation could be brought about in the infinite channel by choosing θ_C^* different from zero in the expansion for θ^*.

We now consider the stability of an established Rossby circulation of the first mode with respect to wave perturbations of the second mode, and vice versa. It may be anticipated that sufficiently near the heavy curve "1" in Fig. 1, the Rossby circulation of the first mode will differ only slightly from the Hadley circulation. If this is actually so, it should be stable with respect to waves of the second mode. If, near the heavy curve "2", the Rossby circulation of the second mode differs only slightly from the Hadley circulation, it should be unstable with respect to waves of the first mode.

If an established steady Rossby circulation of the first mode is regarded as known, equations (34)–(36), and the three equations obtained by eliminating ω_C, ω_M, and ω_N from (40)–(42) and (47)–(49), form a set of six linear homogeneous equations in the six unknowns ψ_C, θ_C, ψ_M, θ_M, ψ_N, and θ_N. The coefficients in these equations are functions of the known solution, and are therefore not independent of time. The vanishing of the real part of an eigenvalue of the matrix of coefficients is therefore not a suitable criterion for the stability of the known circulation.

To overcome this difficulty, we introduce the variables

$$\psi_{K0}=B^{-1}(\psi_K\psi_K+\psi_L\psi_L)=B, \tag{68}$$

$$\theta_{K0}=B^{-1}(\psi_K\theta_K+\psi_L\theta_L)=pB, \tag{69}$$

$$\psi_{L0}=B^{-1}(\psi_K\psi_L-\psi_L\psi_K)=0, \tag{70}$$

$$\theta_{L0}=B^{-1}(\psi_K\theta_L-\psi_L\theta_K)=-qB, \tag{71}$$

$$\psi_{M0}=B^{-1}(\psi_K\psi_M+\psi_L\psi_N), \tag{72}$$

$$\theta_{M0}=B^{-1}(\psi_K\theta_M+\psi_L\theta_N), \tag{73}$$

$$\psi_{N0}=B^{-1}(\psi_K\psi_N-\psi_L\psi_M), \tag{74}$$

$$\theta_{N0}=B^{-1}(\psi_K\theta_N-\psi_L\theta_M). \tag{75}$$

These variables may be regarded as coefficients in new expansions for ψ and θ, in a coordinate system moving with the wave of the first mode. For the established steady Rossby circulation of the first mode, $\dot{B}$ vanishes, while $\dot{\psi}_K=-\omega\psi_L$, $\dot{\theta}_K=-\omega\theta_L$, $\dot{\psi}_L=\omega\psi_K$. and $\dot{\theta}_L=\omega\theta_K$. The superposed quantities ψ_C,θ_C, ψ_{M0},θ_{M0}, ψ_{N0}, and θ_{N0} are then governed by a set of six homogeneous linear equations, which are formally identical with the equations governing ψ_C,θ_C, ψ_M, θ_M, ψ_N, and θ_N, except for the *additional* terms $\dot{\psi}_{M0}=\omega\psi_{N0}$, $\dot{\theta}_{M0}=\omega\theta_{N0}$, $\dot{\psi}_{N0}=-\omega\psi_{M0}$, $\dot{\theta}_{N0}=-\omega\theta_{M0}$. The matrix $\mathfrak{M}$ of the coefficients of these equations is given by

$$k^{-1}\mathfrak{M}=\begin{Bmatrix} -1 & 1 & 0 & \frac{3}{4}qX & \frac{3}{4}X & \frac{3}{4}pX \\ \frac{4\sigma}{1+4\sigma} & -\frac{1+8\sigma}{1+4\sigma} & -\frac{1-3\sigma}{1+4\sigma}qX & 0 & -\frac{1-3\sigma}{1+4\sigma}pX & \frac{1+3\sigma}{1+4\sigma}X \\ 0 & \delta' qX & -1 & 1 & -\frac{4}{5}\beta' G+\frac{\omega}{k} & -\frac{4}{5}\beta' G \\ \frac{1+\delta' s'}{1+s'}qX & 0 & \frac{s'}{1+s'} & -\frac{1+2s'}{1+s'} & \frac{4}{5}\frac{1-\beta' s'}{1+s'}G & -\frac{4}{5}\frac{1+\beta' s'}{1+s'}G+\frac{\omega}{k} \\ \delta' X & \delta' pX & \frac{4}{5}\beta' G-\frac{\omega}{k} & \frac{4}{5}\beta' G & -1 & 1 \\ \frac{1+\delta' s'}{1+s'}pX & -\frac{1-\delta' s'}{1+s'}X & -\frac{4}{5}\frac{1-\beta' s'}{1+s'}G & \frac{4}{5}\frac{1+\beta' s'}{1+s'}G-\frac{\omega}{k} & \frac{s'}{1+s'} & -\frac{1+2s'}{1+s'} \end{Bmatrix} \tag{76}$$

where $X=k^{-1}\alpha''B$ and $s'=(1-\beta')^{-1}\sigma_0$, and the subscript "0" has been omitted from σ_0. The elements of $\mathfrak{M}$, although dependent upon the particular Rossby circulation of the first mode, do not vary with time. The criterion for stability is therefore the vanishing of the real part of an eigenvalue of $\mathfrak{M}$.

The eigenvalues are the roots of the characteristic equation

$$\sum_{j=0}^{6} c_j\lambda^j=0 \tag{77}$$

obtained by equating the determinant $|\mathfrak{M}-\lambda I|$ to zero. In particular, $c_6=1$, and $c_0=|\mathfrak{M}|$. Because of the particular locations in $\mathfrak{M}$ of the elements which contain X, c_6 and c_5 are independent of X, c_4 and c_3 are linear functions of X^2, while c_2, c_1, and c_0 are quadratic functions of X^2. In general the coefficients c_j are complicated algebraic functions of σ_0. Ultimately, they depend upon $\theta_A{}^*$ and k.

If values of $\theta_A{}^*$ and k are found for which the eigenvalues of $\mathfrak{M}$ all have negative real parts, and then $\theta_A{}^*$ and k are allowed to vary continuously, equation (77) may eventually acquire either a real positive root or a pair of complex conjugate roots with positive real parts. In the former case, (77) will first acquire a zero root, and, in the latter case, pure imaginary roots.

The condition for a zero eigenvalue of $\mathfrak{M}$ is that

$$c_0=0 \tag{78}$$

since c_0 is the product of the roots of (77). The condition for a pair of pure imaginary eigenvalues (provided that there are no eigenvalues with positive real parts) is that the left side of (77) have a factor λ^2+a^2, where $a\neq 0$. The sum of the terms of even degree in (77), and also the sum of the terms of odd degree, must then each have the factor λ^2+a^2, so that

$$\sum_{j=0}^{2}(-a^2)^j c_{2j+1}=0, \tag{79}$$

$$\sum_{j=0}^{3}(-a^2)^j c_{2j}=0. \tag{80}$$

Multiplying equations (79) and (80) by $-a^2$, and multiplying equation (79) by a^4, we obtain [with (79) and (80)] a set of five linear homogeneous equations in the quantities 1, $-a^2$, a^4, $-a^6$, a^8. The condition that these equations be consistent is the vanishing of the determinant D of the coefficients;

$$D\equiv\begin{vmatrix} c_1 & c_3 & c_5 & 0 & 0\\ c_0 & c_2 & c_4 & c_6 & 0\\ 0 & c_1 & c_3 & c_5 & 0\\ 0 & c_0 & c_2 & c_4 & c_6\\ 0 & 0 & c_1 & c_3 & c_5 \end{vmatrix}=0. \tag{81}$$

The coefficients c_j, and hence the determinant D, are readily computed for numerical values of σ and X. Because the coefficients c_j vary at most quadratically with X^2, they may, for any one value of σ, be determined for all values of X^2 as linear combinations of their values for three particular values of X^2.

In Fig. 1, the thin solid curve labeled "1" is given by the condition $c_0=0$. The curve $D=0$ lies far to the right of this curve, and is not shown in Fig. 1. The curve $c_0=0$ is therefore the criterion for the stability of a Rossby circulation of the first mode. Between the two curves labeled "1", a stable Rossby circulation of the first mode may exist.

It appears, then, that among the mathematically possible circulations of the first mode, only a small portion are actually stable, and would be expected to occur in a physical experiment. The region of stability would presumably be further altered in a less highly truncated model.

Considering now the stability of an established circulation of the second mode with respect to perturbations of the first mode, we find that if new variables ψ_{K0}', θ_{K0}', $\cdots$are defined by equations analogous to (68)–(75), the variables ψ_C, θ_C, ψ_{K0}', θ_{K0}', ψ_{L0}', θ_{L0}' are governed by six homogeneous linear equations whose matrix of coefficients $\mathfrak{M}'$ is given by

$$k^{-1}\mathfrak{M}'=\begin{Bmatrix} -1 & 1 & 0 & -\frac{3}{4}q'X' & -\frac{3}{4}X' & -\frac{3}{4}p'X'\\ \dfrac{4\sigma}{1+4\sigma} & -\dfrac{1+8\sigma}{1+4\sigma} & -\dfrac{1+3\sigma}{1+4\sigma}q'X' & 0 & -\dfrac{1+3\sigma}{1+4\sigma}p'X' & \dfrac{1-3\sigma}{1+4\sigma}X'\\ 0 & \delta q'X' & -1 & 1 & -\frac{5}{4}\beta G'+\dfrac{\omega'}{k} & -\frac{5}{4}\beta G'\\ \dfrac{1+\delta s}{1+s}q'X' & 0 & \dfrac{s}{1+s} & -\dfrac{1+2s}{1+s} & \dfrac{5}{4}\dfrac{1-\beta s}{1+s}G' & \dfrac{5}{4}\dfrac{1+\beta s}{1+s}G'+\dfrac{\omega'}{k}\\ \delta X' & \delta p'X' & \frac{5}{4}\beta G'-\dfrac{\omega'}{k} & \frac{5}{4}\beta G' & -1 & 1\\ \dfrac{1+\delta s}{1+s}p'X' & -\dfrac{1-\delta s}{1+s}X' & \dfrac{5}{4}\dfrac{1-\beta s}{1+s}G' & \dfrac{5}{4}\dfrac{1+\beta s}{1+s}G'-\dfrac{\omega'}{k} & \dfrac{s}{1+s} & -\dfrac{1+2s}{1+s} \end{Bmatrix} \tag{82}$$

where $X'=k^{-1}\alpha''B'$. The coefficients c_j' of the characteristic equation of $\mathfrak{M}'$, and the determinant D' defined by a relation analogous to (81), may again be readily computed numerically.

Again in Fig. 1, the thin solid curve labeled "2" is given by the condition $c_0'=0$. In this case it is the region on the concave side where the Rossby circulation of the second mode is stable with respect to perturbations of the first mode. In the area between the two thin solid curves, neither a steady Rossby circulation of the first mode nor one of the second mode is stable with respect to all possible perturbations.

The dashed curve labeled "2" is composed of segments of two intersecting curves where $D'=0$. On the convex side of this curve, small disturbances of a suitable shape, superposed upon a Rossby circulation of the second mode, will amplify in an oscillatory manner. To the right of the point where this curve intersects the curve $c_0'=0$ there is a region where oscillatory instability, or "overstability," will initially be preferred over nonoscillatory instability.

In summary we have established the existence of a stable Hadley regime for suitable values θ_A^* and k^{-1}. For certain other values of θ_A^* and k^{-1}, one or the other of two qualitatively different Rossby regimes, each having but one degree of freedom, exists and is stable. Finally, there are values of θ_A^* and k^{-1} for which neither of the above Rossby regimes is stable, although either one exists mathematically.

These considerations demand the existence of solutions in which waves of the first and second modes exist simultaneously. Such solutions do not necessarily have more than one degree of freedom, since it is possible that waves of each mode move together with equal speeds, each maintaining a constant amplitude. Indeed, the occurrence of a single real positive eigenvalue of $\mathfrak{M}$ or $\mathfrak{M}'$, rather than complex conjugate eigenvalues, for values of θ_A^* and k^{-1} for which the Rossby flow of one mode or the other is slightly unstable, suggests, but by no means proves, that the finite-amplitude solutions for these values of θ_A^* and k^{-1} also will be nonoscillatory when viewed in a moving coordinate system. Steady Rossby circulations in which waves of each mode move together without changing their form will be called *Rossby circulations of mixed mode.*

Conceivably, it is possible to solve analytically for all Rossby circulations of mixed mode. If any such solution can be found, it can be tested for stability with respect to further perturbations, in the manner in which we have tested the simpler Rossby solutions for stability. If it proves to be unstable for values of θ_A^* and k^{-1} for which the simpler Rossby flows and the Hadley flow are also unstable, the existence of solutions with at least two degrees of freedom will be proven. Even in this case, the existence of stable vacillating solutions will not be established, since the solutions with exactly two degrees of freedom, if they exist, may themselves be unstable with respect to still further disturbances.

In any event, the contemplated procedure is extremely cumbersome, involving, among other things, the evaluation of fourteenth order determinants. It would therefore seem that the existence of vacillation may be most readily established by using numerical integration procedures to determine particular time-dependent solutions.

5. Numerical solutions

In this section we shall summarize the principal features of a large number of explicit time-dependent solutions of equations (31)–(50), obtained by stepwise numerical integration. The equations are ordinary differential equations, so that finite-difference approximations are needed only to represent the time derivatives. In all our computations we have used the double-approximation procedure, where the value of a variable at a particular iteration is obtained by averaging the value at the previous iteration with the result of two successive uncentered forward extrapolations. This procedure has been discussed in detail by the writer (1963); it may be applied to many nonconservative systems for an unlimited number of iterations, without computational blow-up.

It is to be anticipated that the higher the Rossby number, the more rapidly waves of either mode will progress. A time-step Δt small enough to insure computational stability when θ_A^* is large is therefore much too small for economy when θ_A^* is small. To avoid computational instability without unnecessary waste of time, we have chosen the value $\Delta t=0.16(\theta_A^*)^{-1}$ for all the computations. In most cases, with this value of Δt, a wave will progress through one wavelength in from twenty to thirty iterations.

All of the numerical integrations have been performed on a Royal McBee LGP-30 electronic computing machine. With the program used, about ten seconds are required for one iteration.

Table 1 has been prepared by the computer. It presents a particular numerical solution of equations (31)–(50). Values of all the variables appear at every fifth iteration N. The values are printed to four decimal places (they are carried in the memory of the machine to about seven places), and the decimal point is omitted.

For this solution, $\theta_A^*=0.25$ and $k=0.30$. According to Fig. 1, the Hadley circulation corresponding to these values is unstable with respect to waves of the first mode, but stable with respect to waves of the second mode. The Rossby circulation of the first mode is unstable with respect to waves of the second mode. It is therefore to be expected that waves of both modes will be present in the solution,

For initial conditions we have chosen a weak zonal circulation, with weak superposed wave disturbances

TABLE 1. Numerical integration of equations (31)–(50) for the case $\theta_A^*=0.25$, $k=0.300$. Variables are observed in fixed coordinate system.

N	ψ_A	ψ_K	ψ_L	ψ_C	ψ_M	ψ_N	$\theta_0-\theta_0^*$	θ_A	θ_K	θ_L	θ_C	θ_M	θ_N	σ_0
0000	0100	0050	0000	0000	0000	0050	0100	0100	0000	0000	0000	0000	0000	0100
0005	0696	0023	0000	0000	−0001	0022	0132	1544	0003	−0012	0000	0008	0003	0223
0010	1435	0023	0007	0000	−0006	0016	0247	2069	0012	−0014	0000	0007	0008	0377
0015	1903	0014	0030	0000	−0015	0007	0359	2258	0025	0000	0000	−0000	0010	0459
0020	2150	−0027	0037	0001	−0014	−0008	0437	2328	0016	0031	0000	−0009	0004	0500
0025	2270	−0063	−0017	0001	0001	−0016	0485	2354	−0032	0037	0000	−0007	−0005	0523
0030	2325	−0004	−0092	0001	0015	−0005	0514	2362	−0062	−0027	0000	0002	−0008	0538
0035	2348	0121	−0040	0002	0009	0011	0533	2362	0013	−0093	0000	0008	−0000	0549
0040	2356	0096	0147	0002	−0007	0012	0547	2358	0128	−0014	−0000	0003	0007	0560
0045	2354	−0161	0178	0003	−0013	−0003	0559	2348	0062	0163	−0000	−0005	0005	0573
0050	2345	−0287	−0149	0003	−0001	−0013	0573	2331	−0190	0133	−0000	−0006	−0003	0591
0055	2327	0093	−0414	0004	0011	−0004	0593	2303	−0228	−0196	−0001	0002	−0006	0618
0060	2299	0538	−0021	0005	0007	0009	0621	2262	0167	−0334	−0001	0006	0000	0655

of each mode. Without some waves present initially, there is no mechanism by which waves could ever form, since the small irregularities inevitably present in laboratory experiments have not been built into the simplified equations.

Observing first the behavior of ψ_A, θ_0, θ_A, and σ_0, we see that the zonal circulation develops rapidly, and, by step 40, approximates the equilibrium Hadley circulation, in which, according to (51)–(54), $\psi_A=\theta_A=0.2367$ and $\theta_0-\theta_0^*=\sigma_0=0.0560$. Meanwhile, observing ψ_K, ψ_L, θ_K, and θ_L ,we see that the wave disturbance of the first mode, which decays rapidly at first, ceases to decay by step 10, and, by step 25, when the zonal circulation is well established, surpasses its initial strength. Thereafter it grows rapidly, apparently at the expense of the zonal flow. The wave disturbance of the second mode, indicated by the remaining variables, decays rapidly at first, and then more slowly, but shows no signs of rejuvenation by step 60.

The successsion of positive and negative values of the variables with subscripts K, L, M, or N reveals the progression of the waves. Evidently the waves are moving through one wave-length in somewhat less than 25 time steps. From the times of sign changes in the various columns, we see that waves of either mode in the field θ lag about five steps behind those in the field of ψ, while, within the field of ψ or θ, waves of the second mode precede those of the first mode by about five steps.

This form of output is not convenient, however, when we wish to examine the progression of values of such quantities as $B=(\psi_K^2+\psi_L^2)^{\frac{1}{2}}$ without further calculation. An alternative form of output prints the values of ψ_{K0}, ψ_{L0}, $\cdots$, as defined by (67)–(74), instead of ψ_K, ψ_L, $\cdots$. Essentially the motion is then viewed in a coordinate system moving with the wave of the first mode.

Table 2 presents the same solution as that given in Table 1, printed in the new form. The values now appear at every tenth iteration, and are rounded off to three places. Values of the last seven variables have been omitted, since they are not needed to identify the regime.

TABLE 2. Numerical integration of equations (31)–(50) for the case $\theta^*=0.25$, $k=0.300$. Variables are observed in moving coordinate system.

N	ψA	ψ_{K0}	ψ_{L0}	ψ_C	ψ_{M0}	ψ_{N0}	$\theta_0-\theta_0^*$
000	010	005	000	000	000	005	010
010	144	002	000	000	000	002	025
020	215	005	000	000	000	002	044
030	233	009	000	000	000	002	051
040	236	018	000	000	001	001	055
050	235	032	000	000	001	001	057
060	230	054	000	001	001	001	062
070	221	075	000	001	001	001	070
080	210	087	000	001	000	001	077
090	203	090	000	002	001	002	081
100	200	090	000	003	001	002	083
110	200	089	000	004	001	003	083
120	200	088	000	005	001	004	083
130	201	088	000	007	002	005	083
140	201	087	000	009	002	007	083
150	202	086	000	012	003	009	083
160	202	084	000	015	004	012	082
170	203	081	000	019	005	015	082
180	204	077	000	022	007	019	081
190	206	072	000	025	008	022	080
200	209	067	000	026	010	024	079
210	211	062	000	026	012	025	078
220	214	059	000	024	013	026	076
230	215	058	000	023	013	025	075
240	216	059	000	022	013	025	075
250	216	060	000	022	013	024	075
260	215	061	000	022	012	024	075
270	215	062	000	023	012	024	075
280	214	062	000	023	012	025	076
290	214	061	000	023	012	025	076
300	215	061	000	023	012	025	076

We see that the equilibrium Hadley circulation, which by step 60 is being upset by the growing wave, does not reestablish itself, but that instead a steady Rossby circulation of the first mode is nearly established by step 100. This circulation is only slightly altered by step 140.

Meanwhile, as revealed by the values of ψ_{M0} and ψ_{N0}, the wave disturbance of the second mode, which at first decays so rapidly, ceases to decay after step 80, and by step 130, when the wave of the first mode is well established, surpasses its initial strength. Thereafter it grows rapidly, apparently at the expense of the wave

of the first mode. By step 220 a new equilibrium is nearly reached; from then until step 300 there is little change in any of the variables. Continuation of the integration for 200 additional steps, not shown in Table 2, shows virtually no further change, indicating that the flow approaches a steady Rossby circulation of mixed mode. Such a circulation was suggested in the previous section.

We note that the final values of ψ_C, ψ_{M0}, and ψ_{N0} are positive. Examination of the governing equations (31)–(50) shows that if two solutions are initially alike except for the signs of those variables with subscripts C, M, and N, they will remain alike except for the signs of these variables. Hence there exists a second stable steady Rossby circulation of mixed mode, characterized by negative values of ψ_C, ψ_{M0}, and ψ_{N0}.

Thus there are two distinct stable circulations of mixed mode, either of which may develop. The initial conditions determine which circulation develops. It is therefore not true, in this case, that the governing equations determine the "climate" uniquely.

In both solutions ψ_A is positive. The "westerly wind," averaged over longitude, is proportional to

$$U=\sqrt{2}\psi_A \sin y+2\sqrt{2}\psi_C \sin 2y. \qquad (83)$$

Hence in the first solution, where $\psi_C>0$, the strongest westerlies lie south of the center of the channel, while in the second solution they lie to the north. In general we may regard $-\psi_C$ as a "zonal index," although it is primarily an index of the position, rather than the intensity, of the zonal westerlies.

In a certain sense the two solutions look much alike, one being obtainable from the other by changing the signs of certain variables. Yet, to a hypothetical inhabitant at a fixed latitude, the local climate will depend very much upon which of the two circulations prevails.

In Table 3, we give the solution corresponding to a somewhat more rapid rotation, with θ_A^* again equal to 0.25 and $k=0.25$. The form is like that of Table 2. At first the zonal flow and the disturbances behave more or less as they did in Table 2, except that developments occur more quickly. But then the variables are unable to find equilibrium values, and continue to oscillate, with a period of about 70 time steps. At step 210, which is nearly a repetition of step 140, the waves of the first mode are very strong and those of the second mode rather weak, while at step 240, which is nearly a repetition of step 170, the waves of the second mode are stronger than those of the first mode. Thus we have obtained a solution which exhibits the phenomenon of vacillation, in this case with a period of 70 time steps.

Throughout the cycle ψ_C remains positive, so that the strongest westerly winds always lie south of the center of the channel, although their latitude fluctuates. There must therefore exist another vacillating solution in which ψ_C remains negative, and the strongest westerly winds remain to the north. Thus there are two distinct vacillating circulations, the choice between them being determined by the initial conditions.

TABLE 3. Numerical integration of equations (31)–(50) the case $\theta_A^*=0.25$, $k=0.250$.

N	ψ_A	ψ_{K0}	ψ_{L0}	ψ_C	ψ_{M0}	ψ_{N0}	$\theta_0-\theta_0^*$
000	010	005	000	000	000	005	010
010	122	003	000	000	000	002	021
020	201	007	000	000	000	003	039
030	227	019	000	001	001	003	049
040	231	046	000	002	002	004	056
050	221	088	000	005	003	005	069
060	198	111	000	012	003	009	084
070	181	109	000	025	006	017	091
080	179	092	000	043	011	030	092
090	188	061	000	051	024	039	089
100	201	039	000	034	041	028	084
110	211	043	000	013	041	014	079
120	215	060	000	004	031	013	077
130	210	084	000	008	019	015	080
140	198	097	000	025	011	022	087
150	189	085	000	045	014	035	090
160	194	053	000	049	029	040	088
170	205	038	000	028	044	021	082
180	213	046	000	009	040	011	078
190	215	066	000	003	028	012	077
200	207	091	000	009	015	015	082
210	194	100	000	027	010	023	088
220	188	083	000	047	015	035	090
230	194	051	000	048	030	039	088
240	206	038	000	026	044	020	082

For the same values of θ_A^* and k, there also exists a pair of *steady* Rossby circulations of mixed mode. An equilibrium solution may be estimated by averaging each variable in the vacillating solution over a vacillation cycle. Choosing this estimate as a new set of initial conditions, computing a new time-dependent solution, averaging this new solution over a vacillation cycle, and then successively repeating this process eventually yields the values 209, 58, 0, 28, 31, 32, 81 for ψ_A, ψ_{K0}, ψ_{L0}, ψ_C, ψ_{M0}, ψ_{N0}, $\theta_0-\theta_0^*$. This solution proves to be unstable; when an approximation to it is used for initial conditions, growing oscillations occur. Thus vacillation has been made possible by the instability of the Rossby solutions of mixed mode.

We note, incidentally, that if we had averaged each variable as measured in the fixed coordinate system, the moving waves would have been averaged out, leaving a zonally symmetric flow in which $\psi_C\neq 0$. Thus, while a long-term average in the moving coordinate system is not itself an exact steady-state solution, a long-term average in the fixed coordinate system does not even resemble a solution.

It is possible to represent any instantaneous state of the system by a point in a fourteen-dimensional phase space, whose coordinates are simply the values of the fourteen variables ψ_A, ψ_K, ψ_L, $\cdots$. Alternatively, we may use a thirteen-dimensional phase space whose coordinates are ψ_A, ψ_{K0}, ψ_C, $\cdots$, since ψ_{L0} is always restricted to be zero. A complete vacillation cycle is then represented by a closed loop in thirteen-dimensional space. The upper right diagram in Fig. 2 shows the

projection of two such loops, one for $\psi_C>0$ and one for $\psi_C<0$, on the plane of ψ_{K0} and ψ_C. The curves have been constructed from the data in Table 3. The stars represent additional statistically stationary (but unstable) solutions. The stars on the ψ_{K0}-axis represent the Hadley circulation and the Rossby circulation of the first mode, while the stars enclosed by the loops represent the Rossby circulations of mixed mode.

The upper left diagram in Fig. 2 is a similar diagram for the conditions of Table 2. Here only the Hadley circulation and the steady Rossby circulations occur, so the diagram contains stars but no curves.

In Table 4, the rotation has again been increased, so that again $\theta_A^*=0.25$, but $k=0.225$. At first the behavior is an accelerated version of that in Table 3, but, by step 90, ψ_C has become negative. Thereafter ψ_C attains extreme values of equal magnitudes but alternating signs, and ψ_{M0} and ψ_{N0} do likewise. Step 240 is nearly a repetition of step 180 except for the signs of ψ_C, ψ_{M0}, and ψ_{N0}; step 180 in turn is nearly a repetition of step 120 except for signs. Thus there is vacillation with a period of about 120 steps.

This vacillation is distinct from that of Table 3, in that changing the signs of ψ_C, ψ_{K0}, and ψ_{L0} does not alter the climate, i.e., the statistical properties of a fully developed solution, but merely shifts the solution in time by about 60 steps. In particular, the mean value of ψ_C is zero, so that the mean latitude of the strongest westerlies is the center of the channel. We shall call the vacillation in this solution *symmetric vacillation*, as opposed to the *unsymmetric vacillation* displayed in Table 3.

The vacillation cycle of Table 4 is represented in the lower left corner of Fig. 2. Here there is a single closed curve instead of two separate loops. The unstable Rossby circulations of mixed mode can still be located. They look somewhat like averages over half a vacillation cycle, but bear no resemblance to averages over a full cycle, even in the moving coordinate system.

Fig. 3 shows symmetric vacillation as the synoptic

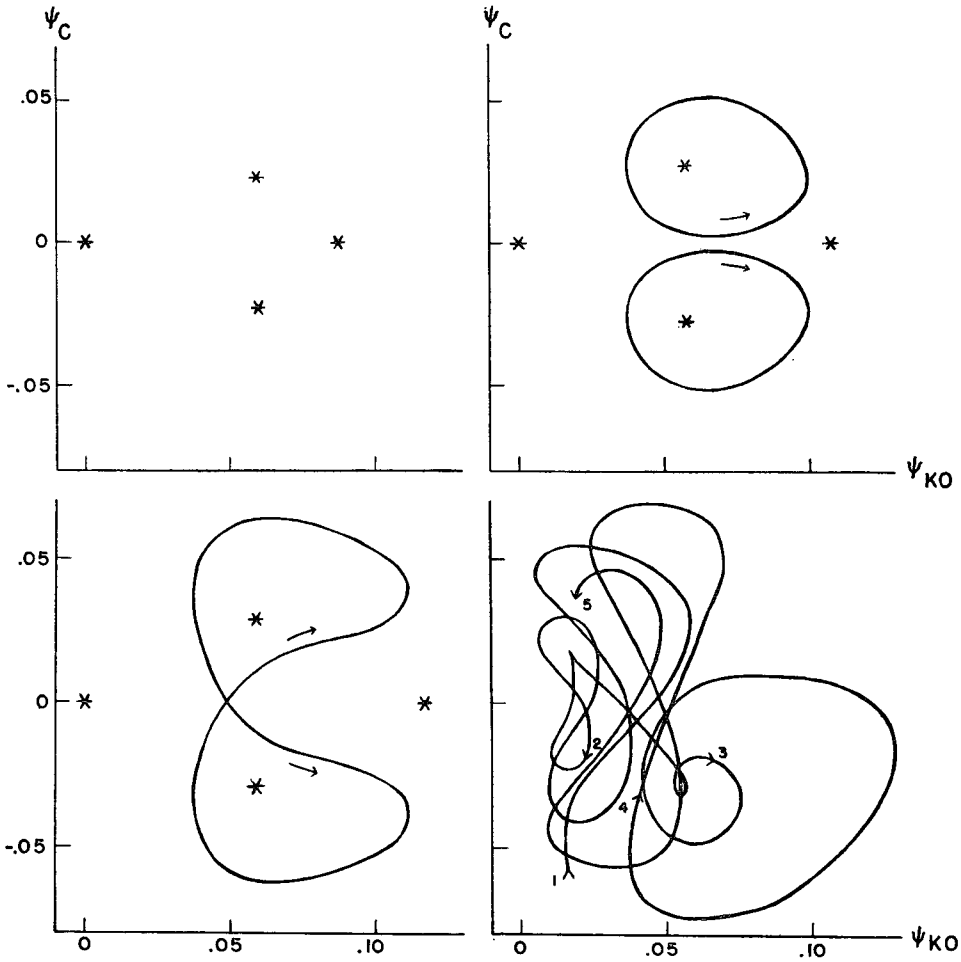

FIG. 2. Projections on the plane of ψ_{K0} and ψ_C of trajectories in phase space. Upper left: $k=0.300$; upper right: $k=0.250$; lower left, $k=0.225$; lower right, $k=0.200$. In all cases $\theta_A^*=0.25$. Stars denote steady Rossby solutions, in most cases unstable. Numbers 1, 2, 3, 4, 5 in lower right indicate time steps 100, 200, 300, 400, 500.

TABLE 4. Numerical integration of equations (31)–(50) for the case $\theta_A^*=0.25$, $k=0.225$.

N	ψ_A	ψ_{K0}	ψ_{L0}	ψ_C	ψ_{M0}	ψ_{N0}	$\theta_0-\theta_0^*$
000	010	005	000	000	000	005	010
010	109	003	000	000	000	002	019
020	190	008	000	000	000	003	036
030	221	026	000	001	002	005	047
040	226	068	000	004	004	007	058
050	205	115	000	015	005	012	079
060	178	115	000	041	009	026	093
070	172	072	000	066	025	044	094
080	187	036	000	040	058	008	089
090	203	048	000	−001	047	−011	083
100	208	069	000	−021	032	−009	081
110	202	094	000	−034	010	−017	085
120	188	092	000	−055	−011	−035	091
130	187	050	000	−060	−041	−040	091
140	199	041	000	−021	−056	006	086
150	207	057	000	010	−042	006	082
160	206	084	000	022	−023	007	082
170	194	106	000	033	−001	017	089
180	180	094	000	056	015	036	094
190	183	048	000	059	043	038	092
200	198	041	000	019	055	−005	086
210	207	058	000	−010	041	−005	082
220	206	085	000	−021	022	−006	082
230	193	108	000	−031	001	−016	089
240	179	097	000	−054	−014	−034	095

meteorologist would look at it. Maps of the field of ψ are given at intervals of twenty time steps. The maps correspond to times steps 130, $\cdots$, 230 in Table 4. The oscillations in the configurations of the trough and ridge lines, and the accompanying shifts in the latitude of the strongest westerlies, are easily observed.

Table 5 presents a final solution, in which θ_A^* again equals 0.25, and $k=0.20$. This time neither symmetric nor unsymmetric vacillation can establish itself. The extreme values of ψ_C, beginning at step 60, are of alternate sign but decreasing magnitude. Then, at steps 270 and 320, two extremes of the same sign are reached; beginning at step 390, the extremes again alternate signs and decrease in magnitude. Between steps 100 and 250, waves of the first mode are generally weak, but they become very strong at step 370. Step 480 is to some extent a repetition of step 140, with the signs of ψ_C, ψ_{M0}, and ψ_{N0} changed, but not a very close repetition. What we have is a solution with at least three degrees of freedom, in regime $\mathcal{R}_{3+}$.

The excursion through phase space, from step 100 to step 500, is shown in the lower right diagram in Fig. 2. The apparent aimless wandering presents a striking contrast to the simple vacillation cycles in the upper right and lower left diagrams.

It thus appears that a given pair of values θ_A^* and k can lead to one of seven distinct regimes of flow: a Hadley circulation; a steady Rossby circulation with waves of the first mode only, both modes together, or the second mode only; unsymmetric or symmetric vacillation; or an irregular nonperiodic flow with at least three degrees of freedom.

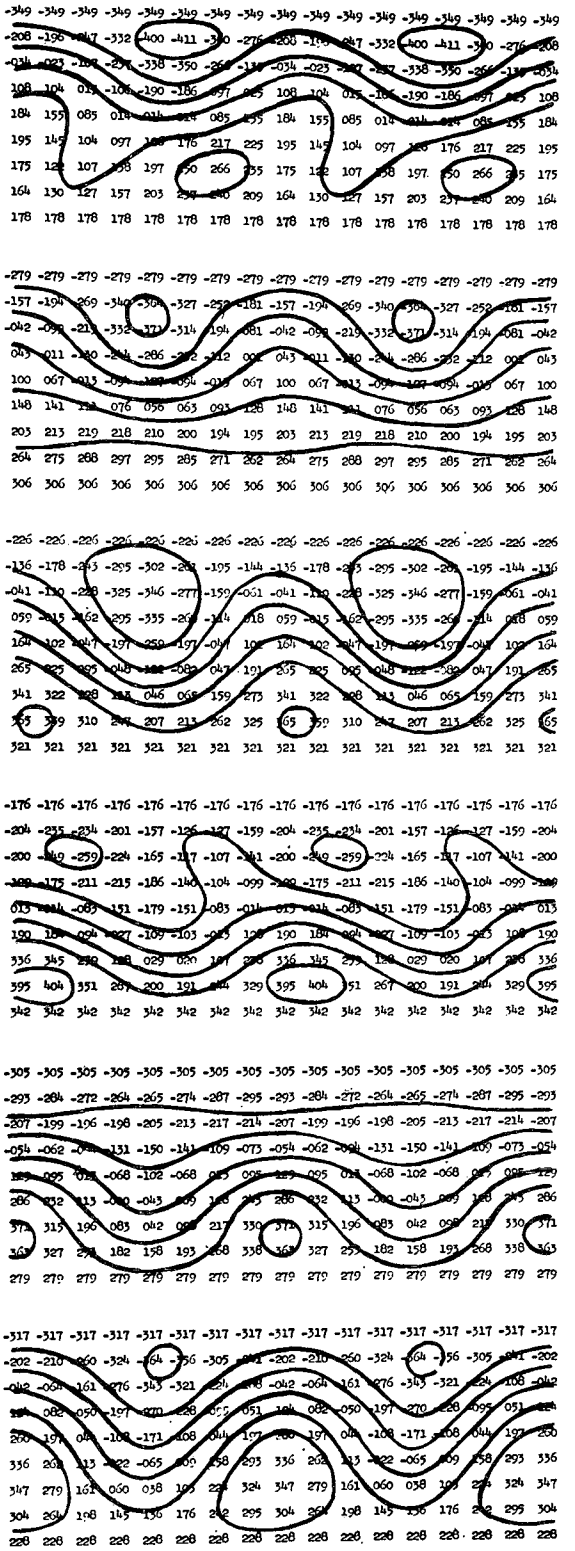

FIG. 3. Field of ψ, at intervals of 20 time steps, for one vacillation cycle, in the case of symmetric vacillation ($\theta_A^*=0.25$, $k=0.225$). Two complete wavelengths in the x-direction are shown. Spacing of streamlines is 0.12 dimensionless units.

TABLE 5. Numerical integration of equations (31)-(50) for the case $\theta_A^*=0.25$, $k=0.200$.

N	ψ_A	ψ_{K0}	ψ_{L0}	ψ_C	ψ_{M0}	ψ_{N0}	$\theta_0-\theta_0^*$
000	010	005	000	000	000	005	010
010	096	003	000	000	000	003	017
020	178	010	000	000	001	004	033
030	214	034	000	002	003	007	045
040	217	093	000	011	006	012	062
050	187	125	000	042	009	027	088
060	166	070	000	082	034	050	096
070	178	047	000	029	057	−032	091
080	192	062	000	−029	041	−031	087
090	196	057	000	−057	024	−039	086
100	201	017	000	−058	−010	−056	085
110	208	036	000	−011	−027	053	082
120	208	045	000	039	−021	056	083
130	207	006	000	045	−009	065	084
140	210	034	000	000	011	−063	082
150	209	029	000	−037	003	−066	083
160	210	010	000	−024	−046	051	083
170	211	027	000	015	−024	062	082
180	211	010	000	029	−036	057	082
190	213	018	000	007	−009	−066	081
200	213	023	000	−019	−013	−065	081
210	212	011	000	−020	−062	−029	082
220	213	018	000	002	−057	036	081
230	213	018	000	016	−063	016	081
240	214	024	000	011	−055	−030	080
250	214	039	000	−005	−045	−040	080
260	211	053	000	−020	−044	−039	082
270	206	057	000	−029	−047	−037	085
280	202	054	000	−029	−053	−032	087
290	201	056	000	−021	−054	−025	087
300	201	066	000	−019	−046	−027	087
310	197	076	000	−032	−038	−035	089
320	192	062	000	−048	−044	−043	092
330	195	043	000	−031	−064	−014	090
340	201	052	000	−001	−056	000	086
350	202	078	000	011	−038	−005	085
360	192	115	000	004	−014	−007	091
370	169	130	000	−016	−004	−012	100
380	154	115	000	−047	−009	−028	101
390	158	063	000	−074	−033	−046	098
400	179	042	000	−031	−059	021	091
410	194	059	000	020	−044	024	087
420	198	071	000	047	−026	028	086
430	196	053	000	069	005	050	088
440	200	030	000	040	059	−024	087
450	204	054	000	−021	041	−039	085
460	203	046	000	−053	031	−042	085
470	206	009	000	−048	053	−022	082
480	212	038	000	−005	005	057	079
490	210	046	000	039	011	060	083
500	207	020	000	037	068	018	085

Fig. 4 is in a sense the principal product of this study. It presents the results of a large number of numerical integrations of the equations. Corresponding to each pair of values of δ_A^* and k for which an integration was performed, a symbol appears in the figure, indicating the regime of flow which occurred. On the basis of these symbols, curves have been drawn separating the regimes. Except for the general suggestion that the curves should be smooth, and concave toward the right, Fig. 1 has not been used to construct the lines in Fig. 4; however, Fig. 1 was used as a guide in choosing some of the values of θ_A^* and k for which integrations were performed.

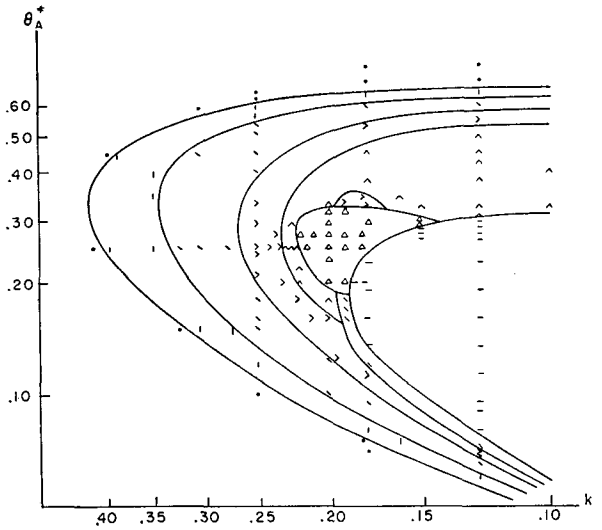

FIG. 4. Critical curves for transitions between regimes of flow. Coordinates are Taylor number and imposed thermal Rossby number. Location of each symbol indicates location of a single numerical solution. Type of symbol indicates regime of flow which occurs. Symbols ⊖ | \ — > ∧ △ denote, respectively, Hadley flow, Rossby flow of first mode, Rossby flow of mixed mode, Rossby flow of second mode, unsymmetric vacillation, symmetric vacillation, and irregular nonperiodic flow.

When an initial state, or an intermediate state, represents a steady solution with superposed small perturbations, it is relatively easy to tell by inspecting the numerical solution whether or not the perturbations are growing. In the central portion of Fig. 4, however, some of the critical curves separate pairs of solutions neither of which is steady, even in the moving coordinate system. The closer one is to a critical curve, the longer the integration may have to be extended to identify the regime with reasonable certainty. Hence, with any prespecified amount of computation, the locations of some of the curves in Fig. 4 will remain somewhat indistinct.

Moreover, parallel to the critical curve for the stability of the steady Rossby flow of the second mode, there is a rather narrow band for which this flow and a more complicated flow are alternative possible stable solutions. Only the more complicated flow is shown in Fig. 4. No attempt has been made to determine whether this phenomenon is a real feature of equations (31)-(50), or whether it results from the finite differencing process.

We see that the regions in Fig. 4 occupied by the Hadley regime, and the Rossby regimes of the first and second modes, are in good agreement with Fig. 1. As suggested in the previous section, the Rossby circulation of the first mode is bounded on the right by the Rossby circulation of mixed mode. The Rossby circulation of the second mode is, however, bounded in part by symmetric vacillation and irregular flow. Apparently, if any Rossby circulation of mixed mode in this portion of the diagram is possible, it is itself unstable with respect to further disturbances. It should be noted in this connec-

tion that the curves $c_0'=0$ and $D'=0$ in Fig. 1 are in close proximity in this region.

Perhaps the most outstanding feature of Fig. 4 is the large number of changes of regime which may occur when the imposed thermal Rossby number and the Taylor number vary over a rather small range. The existence of so many regimes suggests some of the difficulties which one might encounter in trying to deduce the climate, or the statistical properties of the flow, directly from the governing equations, without resorting to numerical integration. An analytic procedure involving only the long-term statistics of the flow might yield the statistics of one of the simpler unstable flows instead of the one which actually develops.

The details of Fig. 4, of course, depend upon the choice of wave number, $n=2$. For other values of n, the central region representing irregular flow might be much larger, or it might even be absent altogether.

We note that as one progresses from left to right in Fig. 4, i.e., as the Taylor number increases, the flow at first becomes successively more complicated. This feature seems to be in agreement with experimental results. The eventual simplification to a steady Rossby circulation of the second mode, at the extreme right of the diagram, appears to have no experimental counterpart, and instead seems to be a result of truncating the governing equations (31)–(50) to include waves of only two modes. If still higher modes had been allowed, they would presumably have become active at Taylor numbers higher than those required to activate the first and second modes.

Finally, we have made no attempt to combine two different wavelengths in the x-direction. Such a step might also yield more complicated flow patterns at high rates of rotation.

6. Unsymmetric and symmetric vacillation

The transitions from Hadley flow to Rossby flow of the first mode, from Rossby flow of the first mode to Rossby flow of mixed mode, and from Rossby flow of mixed mode to unsymmetric vacillation, as the Taylor number continually increases, represent in each case the critical conditions for the instability of the simpler flow with respect to motion characteristic of the more complicated flow. Indeed, all of these simpler flows are mathematically possible, but unstable, when unsymmetric vacillation occurs. It is not obvious, however, how the transition between unsymmetric and symmetric vacillation can be identified with the instability of either type of flow with respect to motions characteristic of the other type. We shall therefore examine this transition in more detail.

In Fig. 5, vacillation cycles resulting from two nearly equal Taylor numbers have been superposed. As in Fig. 2, the coordinates are ψ_{K0} and ψ_C. For the lower rotation, where $\theta_A^*=0.25$ and $k=0.233$, unsymmetric vacillation occurs. Only one of the two possible loops is shown. For the higher rotation, where $\theta_A^*=0.25$ and $k=0.231$, symmetric vacillation occurs. Successive dots on either curve mark the passage of ten time steps.

Throughout much of the length of the unsymmetric-vacillation curve, the symmetric-vacillation curve nearly coincides with it. However, as the curves pass from left to right past the center of the diagram, they diverge slightly, and pass closely by the point Q, marked by a star, on opposite sides of Q. This point represents the unstable steady Rossby flow of the first mode. (There is really a separate point Q for each Taylor number, but these are indistinguishable in the diagram.) The temporary approach to a steady state is further reflected in the closeness of the dots on the curves, as they pass Q. The instability of the steady state is reflected in the increasing distance between the dots, as the curves leave again.

Sufficiently small departures from the Rossby solution of the first mode, when viewed in the moving coordinate system, are approximately governed by a set of thirteen linearized equations (since $\psi_{L0}\equiv 0$). For a considerable range of values of θ_A^* and k, the matrix of coefficients of these equations possesses a single positive eigenvalue, and twelve eigenvalues with negative real parts. In thirteen-dimensional phase space there is therefore a twelve-dimensional hypersurface H passing through Q, such that trajectories (i.e., time dependent solutions of equations (31)–(50)) which lie in H approach Q asymptotically as $t\rightarrow\infty$. There is also a single curve C passing

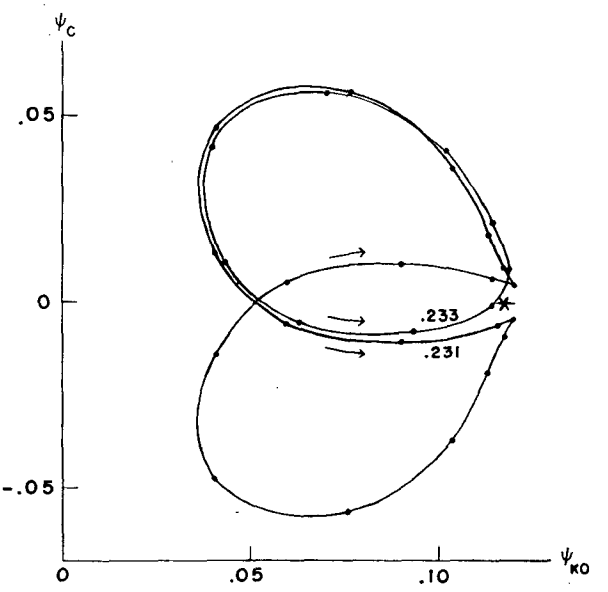

FIG. 5. Projections on the plane of ψ_{K0} and ψ_C of trajectories in phase space, for nearly critical unsymmetric vacillation ($\theta_A^*=.25$, $k=.233$), and nearly critical symmetric vacillation ($\theta_A^*=.25$, $k=.231$). Star denotes location of point Q representing unstable Rossby flow of first mode. Dots on curves are separated by ten time steps.

through Q, such that trajectories passing near Q but not lying in H approach C asymptotically, and leave the vicinity of Q in the (positive or negative) direction of C.

Sufficiently close to Q, H resembles a hyperplane and C resembles a straight line, but farther away, where the linearized equations no longer apply, H and C assume more complicated shapes. For some values of θ_A^* and k, a moving point leaving Q along C never approaches Q closely again. However, the configurations of H and C vary continuously with θ_A^* and k, and, for a given imposed thermal Rossby number, there is one critical Taylor number for which a moving point leaving Q along C finds itself on H, and is steered exactly into Q again. For slightly subcritical rates of rotation, a point moving along C approaches Q closely again, and then departs in the same direction in which it previously departed, nearly repeating its earlier path. For slightly supercritical rates, a moving point approaches Q closely and then departs in the opposite direction from that of its previous departure, only to reverse directions again following its next approach to Q.

The transition from unsymmetric to symmetric vacillation therefore cannot be said to occur because unsymmetric vacillation, although mathematically possible, is unstable for the higher rates of rotation. On the contrary, unsymmetric vacillation does not seem to exist at all when the Taylor number is supercritical. Similarly, symmetric vacillation does not appear to exist when the Taylor number is subcritical, and unsymmetric vacillation cannot be attributed to the instability of symmetric vacillation.

Moreover, the transition does not depend upon the local nature of the instability at Q. Instead, it depends upon the entire large-scale configurations of the curve C and the hypersurface H, both near Q and far-removed from Q.

In Fig. 4 there is another small region of unsymmetric vacillation, just above the region of irregular flow. This vacillation does not resemble the unsymmetric vacillation which we have just examined. It looks more like symmetric vacillation, but its behavior while ψ_C is positive is not quite a mirror image of its behavior when ψ_C is negative. Presumably it does arise from the instability of symmetric vacillation.

Finally, we may inquire about the nature of the transition between symmetric vacillation and irregular flow. Possibly it also results from the instability of symmetric vacillation. It is not easy, however, to locate an unstable vacillating solution by numerical integration, since we cannot, simply by equating certain variables to zero, suppress the additional oscillations which wish to grow upon the vacillating flow. For the time being, then, the existence of unstable vacillating flow, when irregular flow is actually observed, must remain hypothetical.

7. Concluding remarks

Laboratory experiments have demonstrated that when a fluid contained in a circularly symmetric rotating vessel is heated symmetrically, the resulting flow may fall into one of several regimes. These include a Hadley regime $\mathfrak{R}_0$, in which the flow is circularly symmetric and steady, a steady Rossby regime $\mathfrak{R}_1$, in which waves progress at a uniform rate without changing their shape, a vacillating Rossby regime $\mathfrak{R}_2$, in which waves undergo regular periodic changes in shape in addition to their progression, and an irregular Rossby regime $\mathfrak{R}_{3+}$, in which the waves vary nonperiodically. The flow in the earth's atmosphere appears to belong in regime $\mathfrak{R}_{3+}$.

We have reproduced all of these regimes with a simple mathematical model. In this model the vertical dimension is represented by two layers. The flow in either layer consists of a zonal flow, represented by two variables, and superposed waves of two modes, each mode represented by two variables. The temperature field is identified with the vertical wind shear through the thermal wind equation. The over-all mean temperature and the mean static stability are also allowed to vary, bringing the number of variables to fourteen, which are governed by fourteen ordinary differential equations.

Analytic solutions may be obtained for the flow in regimes $\mathfrak{R}_0$ and $\mathfrak{R}_1$, but solutions representing the more complicated flow patterns are best obtained by numerical integration. The central result of this study is presented in Fig. 4, which shows the regimes of flow arising from various values of the imposed thermal Rossby number θ_A^*, used as a measure of heating, and the Taylor number k^{-2}, used as a measure of rotation. Regardless of the value of θ_A^*, a sufficiently low value of k^{-2} leads to a stable Hadley circulation. If θ_A^* is not too large, this Hadley circulation becomes unstable as k^{-2} is increased, and a steady Rossby circulation with waves of the first mode develops. As k^{-2} is further increased, this circulation also becomes unstable, and a steady Rossby circulation with waves of both modes arises. At a still higher Taylor number this circulation too becomes unstable, and a vacillating circulation appears.

Further transitions at still higher rates of rotation are not so readily identified with the instability of the simpler circulation. It is at this point, however, that the model begins to lose some of its resemblance to reality, since still further modes of oscillation, which have been omitted from the model, would, if included in the model, presumably become active at high Taylor numbers.

In a model admitting many modes of oscillation, it seems likely that the regime of flow will continue to become more and more complicated as the rate of rotation continually increases. In this case, the initial appearance of vacillation, as the Taylor number increases from low values, may be ascribed to the instability of the steady Rossby flow. If our hypothesis is correct, the

disappearance of vacillation, as the Taylor number further increases, may be ascribed to the instability of the vacillating motion itself with respect to still further modes of oscillation.

Acknowledgment. The writer is indebted to Miss Ellen Fetter for her indispensible aid in performing and handling the great number of numerical computations needed in this study.

REFERENCES

Fultz, D., R. R. Long, G. V. Owens, W. Bohan, R. Kaylor and J. Weil, 1959: Studies of thermal convection in a rotating cylinder with some implications for large-scale atmospheric motions. *Meteor. Monographs*, 4, No. 21, Boston, Amer. Meteor. Soc., 104 pp.

Hide, R., 1953: Some experiments on thermal convection in a rotating liquid. *Quart. J. R. meteor. Soc.*, **79**, 161.

Lorenz, E. N., 1953: A proposed explanation for the existence of two regimes of flow in a rotating symmetrically-heated cylindrical vessel. Fluid models in geophysics, *Proc. Ist Sympos. on the Use of Models in Geophysical Fluid Dynamics*, Baltimore, 73–80.

——, 1960: Energy and numerical weather prediction. *Tellus*, **12**, 364–373.

——, 1962: Simplified dynamic equations applied to the rotating-basin experiments. *J. atmos. Sci.*, **19**, 39–51.

——, 1963: Deterministic nonperiodic flow. *J. atmos. Sci.*, **20**, 130–141.

Phillips, N. A., 1951: A simple three-dimensional model for the study of large-scale extratropical flow patterns. *J. Meteor.*, **8**, 381–394.

Ward, F., and R. Shapiro, 1961: Meteorological periodicities. *J. Meteor.*, **18**, 635–656.